JOURNAL OF PROPULSION AND POWER
Vol. 14, No. 4, July–August 1998

Slingatron Mass Launchers

Derek A. Tidman*
Slingatron Technologies, Inc., McLean, Virginia 22101

A circular mass-accelerator concept is described in which a projectile of large mass could be accelerated to high velocity using a relatively low-power input (compared to a hypervelocity gun). The machine, called a slingatron, is dynamically similar to the ancient sling, and has a phase stability similar to a modern synchrotron. The projectile slides in a low-friction manner around the accelerator ring using a gas bearing, and work is done on the mass by a phased small-amplitude gyration of the entire accelerator ring. A spiral version of the accelerator (that gyrates with a constant frequency) is also discussed that is phase stable and analogous to a cyclotron. The radius of the ring (or outer ring for the spiral) could range from meters to kilometers, and potential applications include hypervelocity impact research, ground-to-space launch of rocket projectiles, and propulsion.

I. Introduction

A MASS accelerator, called a slingatron, has been proposed in which a mass could be accelerated in an evacuated guide tube around a circular path of large radius to high velocity.[1] The slingatron is similar to both the ancient sling and also to a modern synchrotron in that the mass is accelerated around the accelerator ring by a wave in which the mass has phase stability. Work is done on the mass by a small-amplitude gyration of the entire accelerator ring (like a giant hula-hoop) that continually pulls the mass radially inward against its centrifugal force, and the accelerating force is an example of a Coriolis force. There is no string to break as in a conventional sling and the process is efficient, even though the ring mass is much larger than the accelerated mass. It is analogous to swirling coffee in a cup without a spoon by moving the cup in a small circle. Because the ratio of the ring radius to the small gyration radius is large, huge wave speeds can be implemented mechanically and controlled electronically.

The accelerated mass (called a *sled* or *projectile*) must slide around the accelerator ring with a low-friction coefficient as it is pushed by centrifugal force against the track inside the guide tube. Frictional forces can be made small by either using a lubricating film of gas (a gas bearing) between the sled and the track, or by magnetically levitating the sled above the track. The gas-bearing sled is much easier to engineer and has the advantages that a room-temperature steel track can be used, and higher bearing pressures (and centrifugal forces) are more easily accommodated. It will be emphasized in this paper because magnetic levitation was discussed earlier.[1] We also extend the earlier discussion of the dynamics, phase stability, and efficiency, and consider both ring and spiral slingatrons.

Figure 1 shows the concept for the ring case that is discussed first. Acceleration of the sled can occur provided the synchronized electric motors that drive the small-amplitude gyration are controlled so that at the sled location the guide tube continually moves with a component that is directed inward along the ring radius. Note that the gyration displacement wave travels around the accelerator ring with a speed vR/r, where r and v are the radius and speed of the gyrational motion, respectively, and R is the ring radius. This wave speed is large for $R >> r$, even though the gyration speed v is relatively small, e.g., in the range of 10–100 m/s, for practical mechanical implementation.

There are various ways to implement the ring gyration. Figure 2 shows an example in which drive units distributed around the accelerator ring use inertial energy stored in flywheels to propel the ring plus counterweights around a small gyration circle. Electrically controlled clutches provide for the increase in gyration speed and also for the surge power needed as the sled approaches its final velocity. No further steps are needed in the power train. For some cases, such as the spiral geometry discussed in Sec. III, one could choose to store the inertial energy required for acceleration in the gyrational motion of the ring plus counterweights, in which case the power train becomes even simpler in that flywheels and clutches are not needed.

The accelerator guide tube could have either a circular or noncircular cross section, and Fig. 2 shows the ring as having a curved U-beam geometry. This geometry provides lateral restraint for the sled, and allows easy access for operations such as grinding welds and honing the steel track to a polished finish. A large steel ring could, for example, be constructed out of curved U-beam sections connected together.

The accelerator has a useful range of phase stability over which the sled can be accelerated by a preprogrammed ramp-up of the gyration frequency (Fig. 3). This is discussed in Sec. II.C and and was observed in a small-scale experiment (Fig. 4), in which phase stability allowed a preprogrammed acceleration to be used.

Note that the ring radius R could range from meters to kilometers, depending on the application. The slingatron concept avoids the technical difficulties of electrical pulsed power for such systems because the acceleration process is relatively slow (just as a conventional sling accelerates slowly compared to a conventional or electromagnetic gun). The final surge power is typically $\leq 10^{-2}$ times that of a gun for the same projectile mass and exit velocity. This makes it capable, in principle, of accelerating very large masses to high velocity, possibly including the direct launch of heavy rocket projectiles into space from the Earth's surface.[2,3] A long skinny projectile in the slingatron would experience the centrifugal and accelerating Coriolis force distributed along its length, not just on its base area. Also, extremely high velocity appears achievable for a small unstructured mass sliding on its evaporatively maintained gas bearing (Sec. IV), and may be useful for physics experiments.

Consider next the high centrifugal gees experienced by the sled. First note that defense projectiles can be fired out of guns with >20,000 gees and carry electronics, etc. It is also instructive to relate the centrifugal gees to the bearing pressure be-

Received Nov. 20, 1997; revision received Feb. 8, 1998; accepted for publication March 16, 1998.

*President, Adjunct Professor, George Mason University, Fairfax, VA 22030. Member AIAA.

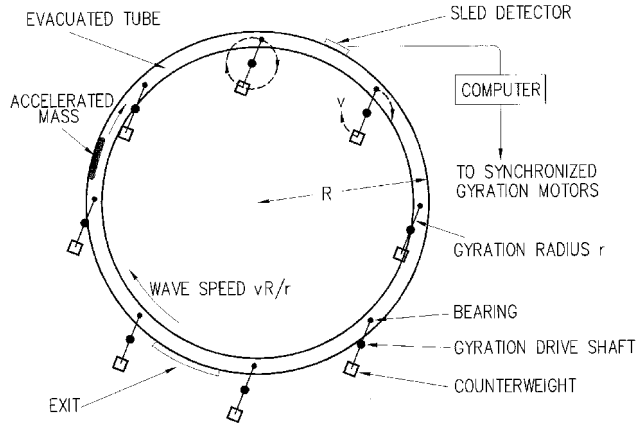

Fig. 1 Accelerator ring of radius R is mounted on gyration drive arms of length $r << R$.

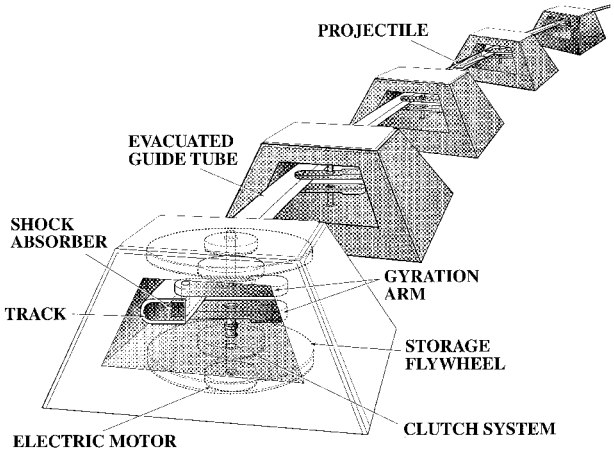

Fig. 2 Gyration energy is supplied by flywheels to the accelerator that in turn transfers energy to the phased projectile.

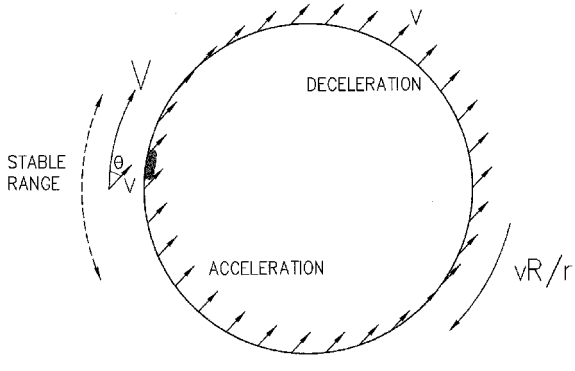

Fig. 3 Schematic showing the gyrating ring velocity v, projectile velocity V, relative phase angle θ, and the stable phase range at a particular instant. The ring displacement travels like a wave of velocity vR/r around the ring.

tween the sled and the track for a sense of what materials or structures can tolerate. For example, 200 bar is easily contained in typical laboratory gas bottles. But 200 bar on one side of a steel slab of thickness 2 in., i.e., ~40 g cm^{-2}, will accelerate the slab at 5000 gees, and 400 bar (also in some gas bottles) will accelerate it at 10,000 gees, which is the centrifugal acceleration experienced by an object traveling at 8 km/s around a circle of radius 640 m. Kilobar bearing pressures could also be used as they are in guns.

In high-velocity light-gas guns it is known that barrel damage can result from collisions between a hypervelocity projectile and microscopic roughness asperities on the polished inner

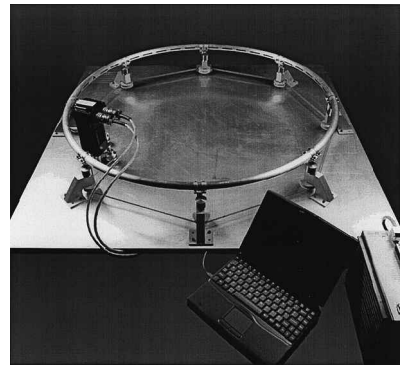

Fig. 4 Table-top slingatron of ring diameter 1 m. The computer-controlled gyration accelerates ball-bearing projectiles to above 100 m/s.

surface of the gun tube. Such collisions cause tear-shaped gouges on the tube's inner surface. Note that the projectile in a gun is typically designed to fit tightly in the barrel to avoid blowby of gas in the beginning of its travel when the propulsive gas pressures are in the several-kilobar range and the projectile velocity is small. However, in the slingatron, a sled's gas bearing can be supplied so that it is much thicker than the height of microscopic asperities on the polished track surface, thereby avoiding asperity collisions with their attendant surface damage. This is important because each slingatron shot involves typically >10 cycles of the sled around the accelerator ring for the last e-folding (exponential increase by a factor e) of the sled's bearing pressure, although only one transit for the spiral version in Sec. III.

Finally, on the issue of efficiency, note first that the gyration power is supplied globally and continuously to the ring as it rolls on bearings with a very low mechanical friction coefficient around its gyration circle. Sled acceleration is efficient because the sled extracts energy from the gyrating ring faster than the ring's bearings dissipate it. Mechanical losses are expected to mainly occur in the clutches. The sled gains a velocity increment of $\sim 2\pi v \sin\theta$ per cycle around the ring, where θ is the angle between the sled and ring velocity vectors. Further, the ratio of the kinetic energy of the sled of mass m to that of the ring system mass M (ring plus counterweights) is $mV^2/Mv^2 \simeq mR^2/Mr^2$, and is usually greater or ~1, in which case less than about half of the energy remains in the ring at the end of the acceleration process. The situation is different for the spiral discussed in Sec. III, but the spiral can function as an inertial energy store in that case and becomes efficient for multiple-shot use.

II. Dynamics

A. Equation of Motion for the Sled

Figure 5 shows a sled of mass m sliding around a circular track of radius R, with the entire track including its center executing a circular motion of radius r. The r at the ring center makes an angle ψ with the x axis in the laboratory frame and the ring R at the sled location makes an angle φ with the x axis. The angle $\psi(t)$ is a given gyration drive function and $\phi(t)$ is the dependent variable determining the sled location. The relative phase angle $\theta = \psi - \phi$ is the angle between the sled and ring velocity vectors (Figs. 3 and 5).

The sled is assumed to slide sufficiently rapidly around the circular track so that it remains on the track. The force $F_\perp$ is the reaction force from the track acting on the sled, and $F_\parallel$ is the frictional force of the track on the sled. These forces act to confine the sled to its circular motion around the track. The equations of motion are thus

$$m\ddot{x} = -F_\perp \cos\phi + F_\parallel \sin\phi$$
$$m\ddot{y} = -F_\perp \sin\phi - F_\parallel \cos\phi \qquad (1)$$

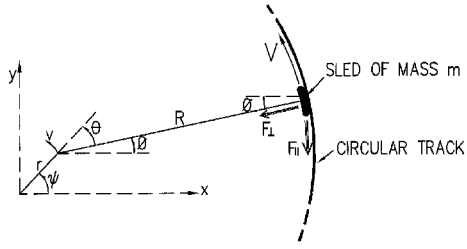

Fig. 5 Parameters for motion of a sled around a gyrating ring in an *xy* coordinate frame fixed in the laboratory.

with the constraints

$$x = R\cos\phi + r\cos\psi, \qquad y = R\sin\phi + r\sin\psi \tag{2}$$

and we assume

$$F_{\parallel} = \mu F_{\perp} \tag{3}$$

where μ is defined as the friction coefficient.

If we solve Eqs. (1) for $F_{\perp}$ and $F_{\parallel}$ and use Eqs. (2) to eliminate $\ddot{x}$ and $\ddot{y}$, and substitute in Eq. (3), the resulting equation of motion for ϕ is

$$R\ddot{\phi} + r\ddot{\psi}\cos(\psi - \phi) - r\dot{\psi}^2\sin(\psi - \phi)$$
$$= -\mu[R\dot{\phi}^2 + r\ddot{\psi}\sin(\psi - \phi) + r\dot{\psi}^2\cos(\psi - \phi)] \tag{4}$$

and the sled speed in the laboratory frame is

$$V = (\dot{x}^2 + \dot{y}^2)^{1/2} = [R^2\dot{\phi}^2 + r^2\dot{\psi}^2 + 2rR\dot{\phi}\dot{\psi}\cos(\psi - \phi)]^{1/2} \tag{5}$$

For acceleration to occur, ψ and ϕ must increase together through many cycles. The acceleration is driven by the small but finite value of r/R, and opposed by the friction coefficient μ. We simplify the equations for solutions of interest by assuming that the quantities r/R, μ, $d^2(\psi, \phi)/dt^2$ are all $\ll 1$, and neglecting second-order terms in these quantities in Eqs. (4) and (5). This gives the approximate equations[1]

$$\ddot{\phi} = (r/R)\dot{\psi}^2\sin(\psi - \phi) - \mu\dot{\phi}^2 \tag{6}$$

$$V \simeq R\dot{\phi} + r\dot{\psi}\cos(\psi - \phi) \tag{7}$$

Note that we require $r/R \ll 1$ so that one can mechanically implement the gyration with a frequency needed to provide a high-speed displacement wave traveling around the ring.

B. Constant Relative-Phase Acceleration

Here we consider the case in which ψ and ϕ increase together through many cycles with a constant relative gyration phase θ

$$\theta = \psi - \phi = \text{const} \tag{8}$$

It follows that $\dot{\psi} = \dot{\phi}$, $\ddot{\psi} = \ddot{\phi}$, and Eqs. (6) and (7) give to first order

$$\dot{V} \equiv g_{\parallel} = g_{\perp}[(r/R)\sin\theta - \mu], \qquad g_{\perp} = V^2/R \tag{9}$$

which was the equation used in Ref. 1. Acceleration occurs provided $r\sin\theta/R > \mu$.

For a gas bearing the friction coefficient derives from viscous drag in the gas film. This drag force is approximately proportional to V^2, as are the centrifugal and coriolis forces. The assumption that μ is constant is thus a reasonable case to consider. Equation (9) can be integrated for constant μ to give

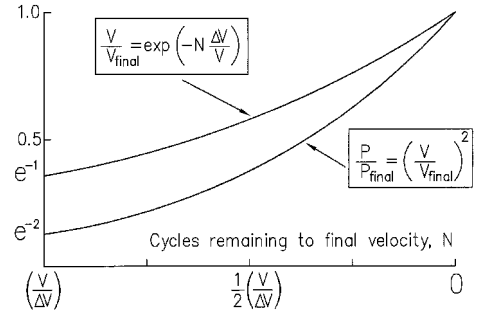

Fig. 6 Graph displaying the projectile's approach to its final velocity in a ring slingatron as a function of the number of cycles remaining to reach final velocity. The gain per cycle is $\Delta V \simeq 2\pi V[(r/R)\sin\theta - \mu]$.

$$V_f = V_i[1 - (\tau_f/\tau_\infty)]^{-1} \tag{10}$$

where τ_f is the acceleration time to velocity V_f, and τ_∞ is the time taken to accelerate to ∞ velocity within this nonrelativistic formulation

$$\tau_\infty(\text{gas}) = R^2/V_i(r\sin\theta - \mu R) \tag{11}$$

and V_i and V_f are the initial and final sled velocities. For this case with both μ and θ constant, the sled's motion is also equivalent to sliding down a potential well, $\Phi + V^2/2 = 0$, with the potential

$$\Phi(x) = -(V_i^2/2)\exp[(2x/R)(r\sin\theta/R - \mu)]$$

Equation (9) can also be solved for constant μ to express the projectile velocity as a function of the number of cycles remaining to reach the projectile's final velocity (Fig. 6).

For a high-velocity magnetically levitated sled, the EM friction coefficient μ has a velocity dependence $V^{-1/2}$. Equation (9) can be simply integrated for this second case to give the acceleration time to reach velocity V_f

$$\tau_f(\text{maglev}) = \frac{2r\sin\theta}{V_i\mu_i^2}\,\ell n\left(\frac{r\sin\theta - \mu_f R}{r\sin\theta - \mu_i R}\right)$$
$$+ 2R\left(\frac{1}{\mu_f V_f} - \frac{1}{\mu_i V_i}\right) \tag{12}$$

where μ_i and μ_f are the initial and final friction coefficients, respectively. For $V_f \gg V_i$ and a small initial friction coefficient, this simplifies to

$$\tau_f \simeq \tau_\infty \simeq R^2/rV_i\sin\theta \tag{13}$$

which is the same as the gas bearing result for small μ.

Multiplying Eq. (9) by mV also gives the energy equation

$$\frac{d}{dt}\left(\frac{1}{2}mV^2\right) = \frac{mV^3}{R}\left(\frac{r}{R}\sin\theta - \mu\right)$$

or, noting for constant θ that $V = v(R/r)$

$$\frac{mV^2}{R}(v\sin\theta) = \frac{d}{dt}\left(\frac{1}{2}mV^2\right) + \mu V\left(\frac{mV^2}{R}\right) \tag{14}$$

From Fig. 5 one can see that the left side of Eq. (14) represents the rate at which work is done on the sled by pulling it radially inward with a speed $v\sin\theta$ against the sled's centrifugal

force mV^2/R. This equals the rate of sled kinetic energy increase plus its friction power loss on the right side of Eq. (14).

C. Stability of Constant Relative-Phase Acceleration

Suppose for example that the sled is undergoing approximately constant phase acceleration with $\theta \sim \pi/4$ and a preprogrammed $\dot{\psi}$ as shown in Fig. 3. If a perturbation causes the sled to speed up, the relative phase θ decreases and the sled's acceleration decreases, causing it to drop back into phase with the gyration wave. Similarly, if the perturbation causes the sled to decrease speed its acceleration increases and the sled tends to catch up with the wave. Because friction is present one expects oscillations about the preprogrammed constant phase acceleration to be damped.

Such phase stability would be useful both for preprogrammed acceleration and for cases in which some degree of feedback control is used. Phase stability was observed experimentally in the small slingatron shown in Fig. 4 in which air drag (also proportional to V^2) was calculated to be the main source of drag.

To examine the dynamics of this we consider the simple case $\mu = \text{const}$ (corresponding approximately to a gas bearing), and use Eq. (6) to examine the evolution of a perturbation from the constant relative phase solution discussed in Sec. II.B. Thus writing

$$\phi = \phi_0 + \phi_1 \tag{15}$$

$$\psi - \phi_0 = \theta = \text{const}, \qquad \dot{\phi}_0/\dot{\phi}_{0i} = (1 - t/\tau_\infty)^{-1} \tag{16}$$

and linearizing Eq. (6) in ϕ_1 leads to

$$\ddot{\phi}_1 + \left[\frac{2\mu\dot{\phi}_{0i}}{1 - (t/\tau_\infty)}\right]\dot{\phi}_1 + \frac{r\cos\theta}{R}\left[\frac{\dot{\phi}_{0i}}{1 - (t/\tau_\infty)}\right]^2 \phi_1 = 0 \tag{17}$$

where $\dot{\phi}_{0i} = \dot{\phi}_0\,(t = 0)$ is the initial value of $\dot{\phi}_0$.

This equation can be solved by making the transformation to an independent variable

$$y = -\ell n[1 - (t/\tau_\infty)] \tag{18}$$

and gives the result for $c > b^2/4$

$$\phi_1(t) = \phi_1(0)\left(1 - \frac{t}{\tau_\infty}\right)^{b/2} \cos\left\{\left(c - \frac{b^2}{4}\right)^{1/2} \ell n\left[\frac{1}{1 - \left(\frac{t}{\tau_\infty}\right)}\right]\right\} \tag{19}$$

where

$$b = \frac{(r\sin\theta + \mu R)}{(r\sin\theta - \mu R)} \tag{20}$$

$$c = \frac{rR\cos\theta}{(r\sin\theta - \mu R)^2} \tag{21}$$

which shows the phase perturbation to have a decreasing amplitude and increasing frequency as a function of time during the acceleration, indicating a useful range of stability inside the quadrant $0 < \theta < \pi/2$. Specifically, noting from Eq. (9) that for acceleration we require $r\sin\theta > \mu R$, and that the solution (19) applies for $c > b^2/4$, it follows that perturbations in the following range are damped:

$$\sin^{-1}\left(\frac{\mu R}{r}\right) < \theta < \frac{\pi}{2} - \frac{r}{4R}\left(1 + \frac{\mu R}{r}\right)^2 \simeq \frac{\pi}{2} \tag{22}$$

However, these range limits are approximate (with particular sensitivity around $\pi/2$) because of the linearization in amplitude and because we used Eq. (6) for the dynamics instead of the exact Eq. (4).

D. Equation of Motion for the Ring

There are various mechanical ways to implement the ring gyration depending on the size of the system, and for purposes of discussion we choose the concept shown in Fig. 2. The ring plus counterweights of total mass $M = 2M_R$ are propelled around the gyration circle by gyration arms that connect through their central shafts to the flywheels via electrically controlled clutches. Most of the mechanical dissipation is expected to be in the clutches with a smaller amount (that we neglect) in the bearings connecting the arms to the ring.[4] There are also shock-absorber units to alleviate the jolt experienced by passage of the sled past the arm-ring connection points.

Forces perpendicular to the rotor arms give a global equation of motion for that part of the system consisting of the gyrating ring plus sled

$$M\dot{v} = F_{\text{drive}} - (mV^2/R)\sin(\psi - \phi) \tag{23}$$

where

$$v = r\dot{\psi}, \qquad M = 2M_R \tag{24}$$

$$F_{\text{drive}} = T_{\text{drive}}/r \tag{25}$$

where v is the gyration speed of the ring, and T_{drive} is the total torque applied by the drive shafts that propel the gyration and generate a total propulsive force F_{drive} around the gyration circle.

Multiplying Eq. (23) by v gives the energy equation for the ring

$$\frac{\mathrm{d}}{\mathrm{d}t}\left(\frac{1}{2}Mv^2\right) = vF_{\text{drive}} - \frac{mvV^2}{R}\sin(\psi - \phi) \tag{26}$$

We have also neglected air drag as the ring gyrates in the atmosphere because that could be minimized by using a shaped outer shell on the ring.

The torque T_{drive} needed to propel the system also follows from Eqs. (9) and (23) as

$$T_{\text{drive}} = rF_{\text{drive}} = \frac{\mathrm{d}}{\mathrm{d}t}(Mvr + mVR) + \mu\left(\frac{mV^2}{R}\right)R \tag{27}$$

E. Efficiency and Mass of the Slingatron

An energy equation for the combined system comprising the ring-counterweight system plus sled now follows by using Eq. (14) in Eq. (26). This gives

$$vF_{\text{drive}} \equiv \varepsilon_{\text{clutch}}\left(\frac{\mathrm{d}W_{\text{fly}}}{\mathrm{d}t}\right) = \frac{\mathrm{d}}{\mathrm{d}t}\left(\frac{1}{2}Mv^2 + \frac{1}{2}mV^2\right) + \mu\left(\frac{mV^3}{R}\right) \tag{28}$$

where $\mathrm{d}W_{\text{fly}}/\mathrm{d}t$ is the electrical power drawn from the flywheels, and $\varepsilon_{\text{clutch}}$ is the efficiency with which this is converted to shaft power to propel the gyration. This power is divided between the hoop system kinetic energy and the sled kinetic energy and its sliding friction loss.

Integrating Eq. (28) over time and using subscripts i for initial and f for final values of parameters gives the energy conservation result

$$\varepsilon_{\text{clutch}}W_{\text{fly}} = \frac{1}{2}M(v_f^2 - v_i^2) + \frac{1}{2}m(V_f^2 - V_i^2) + \int_0^t \mathrm{d}t\left(\frac{\mu m V^3}{R}\right) \tag{29}$$

The integral in Eq. (29) can be evaluated by assuming μ (sled) is constant, and using Eq. (9). If we also assume the initial energy is small compared with the final energy in the system, Eq. (29) gives for the overall efficiency from flywheels to the sled

$$\varepsilon = \varepsilon_{\text{clutch}}\varepsilon_{\text{ring}} \simeq 0.5mV_f^2/(\text{flywheel KE}) \tag{30}$$

where

$$\varepsilon_{\text{ring}} \simeq \left[1 + \frac{Mr^2}{mR^2} + \frac{\mu R}{(r\sin\theta - \mu R)}\right]^{-1} \tag{31}$$

and $\varepsilon_{\text{ring}}$ is the efficiency with which energy supplied by the drive shafts to the ring is transferred to sled kinetic energy (KE).

The last term in Eq. (31) is typically <1 because the accelerating force acting on the sled would usually be a few times the sled's drag force for acceleration to occur. In the limit that $\mu = 0$, the ring efficiency becomes

$$\varepsilon \sim \varepsilon_{\text{clutch}}\left(1 + \frac{Mr^2}{mR^2}\right)^{-1} = \varepsilon_{\text{clutch}}\left(\frac{mV^2}{mV^2 + Mv^2}\right) \tag{32}$$

for which case the energy loss is the energy dissipated in the clutches plus the kinetic energy left in the gyrating ring system at the end of the acceleration process when the projectile is launched. A part of the energy $Mv^2/2$ of the ring-counterweight system may also be recoverable.

A computer simulation of the dynamics of the mechanical system is needed for an accurate calculation of M as a function of the parameters m, V, r/R, etc. As the sled passes a given point it delivers an impulse to the track that would generate various kinds of elastic wave motion in response. Waves of propagation speed less than the sled speed would be left behind and decay in the sled's wake, and waves of higher speed would propagate both ahead and behind the sled.

To obtain an overestimate for the minimum ring mass M_R, we note that the ring is supported by many gyration drive units spaced at intervals of several r around the circumference. Assume that the centrifugal force of the sled $mg_\perp$ is suddenly applied at the midsection of a track segment at time $t = 0$ and then statically held in place for $t > 0$, and that the ends of the track segment are held rigidly in place at the drive units. The span would then deflect and overshoot the static stress experienced at each end of the span, $mg_\perp/2A$, by a factor of 2 before undergoing damped oscillations and finally settling at the static stress value. Writing S for the shear-stress limit of the steel beam[4] gives the shear-limit cross-sectional area $A_{\text{shear}} = mg_\perp/S$ of the beam for this overshoot stress and, thus, from the shear-limit mass for the track $M_R = M/2 \leq 2\pi R\rho_s A_{\text{shear}}$ from which it follows

$$\frac{M_R r^2}{mR^2} = \frac{M_R v^2}{mV^2} \leq 2\pi\left(\frac{v}{v_s}\right)^2 \tag{33}$$

where $v_s = (S/\rho_s)^{1/2}$, and v is the gyration speed. For example, for steel $\rho_s = 8$ gm/cm^3, $S = 12{,}000$ lb/in.$^2 \equiv 8.3 \times 10^8$ dyne/cm^2, and $v_s \simeq 100$ m/s. It also follows that

$$M_R \leq 2\pi mV^2/v_s^2, \qquad A_{\text{shear}} = M_R/2\pi\rho_s R \tag{34}$$

i.e., this maximum ring mass is constant for a given m, V, and the ring cross section A_{shear} (as well as that of the support shafts under the ring and the rotor arms), decreases as R increases. By choosing a large R it becomes mechanically easier to urge the projectile around its circular path without increasing the system mass.

The shear-limit ring mass M_R is an overestimate because the gyration arms would allow for some recoil of the ring via the shock absorbers and clutches as the sled traversed it, i.e., the ring would not be held rigidly in place at the gyration units. Also, the sled delivers a very short impulse $\propto V$ to each section of track it traverses and not a force loading $\propto V^2$ that stays in place once applied. However, based on the overestimate [Eq. (33)] the efficiency $\varepsilon_{\text{ring}}$ given by Eq. (32) is expected to be at least greater than $0.1\varepsilon_{\text{clutch}}$ provided $V < (3v_s/2\pi)(R/r)$.

III. Constant-Frequency Spiral Slingatron

Here we discuss an alternative slingatron geometry in which the guide tube has a spiral shape (Fig. 7), instead of the circular geometry discussed in Sec. II. Drive motors distributed along the spiral are used to establish a constant gyration frequency (with constant gyration radius) before a shot. The projectile is then injected into the inner spiral entrance at velocity V_i and traverses the spiral in phase with the gyration, i.e., with the same cycling frequency, until it exits from the outer ring of the spiral with a final velocity $V_f = V_i(R_f/R_i)$, analogous to a cyclotron. The geometry of the spiral is chosen so that the accelerating projectile maintains its constant cycling frequency while accelerating. Phase stability is physically expected for this case as in the ring, and has been confirmed using a computer simulation of the acceleration.

Several advantages accrue from this variant of the slingatron. Specifically, the spiral version allows one to store the needed energy in the gyrational motion of the track-counterweight system prior to a shot. The projectile draws on this energy as it makes a single pass through the spiral, thus simplifying the power train by eliminating the need for the flywheels and clutches shown in Fig. 2. Further, the spiral has a simple entrance and exit so that no fast doors are needed, except possibly for provision of a vacuum in the guide tube. Barrel wear is reduced because of the single traversal per shot.

For a case where the projectile is gun-injected into the spiral with an initial velocity larger than the speed of the guide-tube mechanical response vibrations, the projectile advances into quiescent track in its pass through. It does not re-encounter its own wake (of either guide-tube modes or bearing gas) as occurs for the circular case. Because the coriolis and drag forces are proportional to mV^2/R, a single spiral geometry could accelerate projectiles of various shapes and masses.

The disadvantage of a spiral slingatron is that the track is long. However, several factors keep the length reasonable. First the inner spirals have smaller ring radii and, thus, also larger values of r/R. This results in velocity gains per cycle comparable to those in the outer spirals, so that not much length is involved in the inner spirals. Typically, the length of the spiral guide tube is about $N/2$ times that of its outer ring. The penalty of increased track length is also offset by the reduction in the power-train mass.

The dynamical equations for a projectile sliding with friction along a gyrating spiral can be obtained by making the follow-

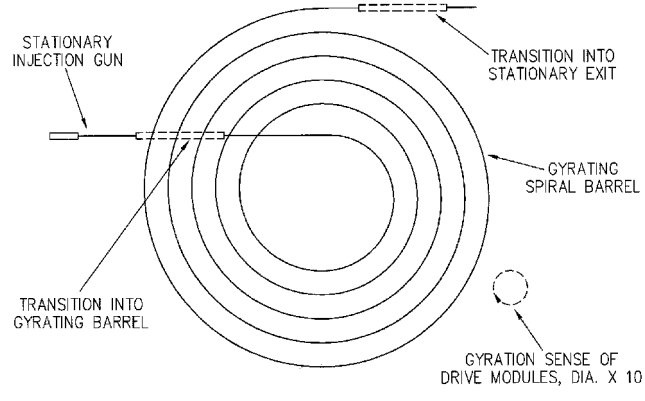

Fig. 7 Spiral slingatron (mass-cyclotron) in which a constant gyration is maintained, and a mass injected into the inner spiral ring emerges with higher velocity from the outer ring.

ing changes to Eqs. (1) and (2). First note that the local radius of curvature $R(\phi)$ is a function of ϕ. Then replace ϕ with $\phi - \beta$ in Eq. (1), but not in Eq. (2), where $\beta = \arctan(R^{-1} dR/d\phi)$. We then seek a solution for the spiral $R(\phi)$ so that a projectile fired into the inner spiral ring traverses the gyrating spiral with the same constant cycling frequency as that of the pre-energized spiral, i.e., assume constant relative phase $\theta = \psi - \phi$, $\psi = \dot{\phi}$, $\dot{\psi} = \ddot{\phi} = 0$. Neglecting terms $\sim r^2$, μr, μ^2, gives

$$R(\phi) = R_i + \mu^{-1}(r \sin\theta - \mu R_i)(1 - e^{-\mu\phi}) \tag{35}$$

$$V = 2\pi R f \tag{36}$$

$$N = \frac{1}{2\pi\mu}\,\ell n\left(\frac{r\sin\theta - \mu R_i}{r\sin\theta - \mu R}\right) \tag{37}$$

$$t(V) = Nf^{-1} \tag{38}$$

where f cps is the constant gyration frequency of the spiral, r and μ are assumed constant, N is the number of turns needed to go from the matched injection velocity V_i to V, and $t(V)$ is the projectile acceleration time through the spiral. Note r/R is relatively large at the injection end of the accelerator but becomes small as R increases (at least for constant μ), so that $r \sin\theta \to \mu R$ and R reaches a maximum value. Also, the impulse per unit length delivered to the guide tube by the projectile as it advances along the spiral, $mV/R = 2\pi mf$, is constant.

Next, we note that the projectile acceleration time through the spiral, N/f, is less than that for the ring accelerator. For example a spiral of 10 turns with a constant gyration frequency of 50 cps would have a projectile acceleration time of 0.2 s. This is advantageous because less gas is required to supply the projectile's low-friction gas bearing during the acceleration.

For a spiral slingatron with a low gyration rate it is simpler to mount the projectile injector mechanism on the gyration platform at the entrance to the inner spiral. However, if the pre-established constant gyration frequency is high, e.g., $f >$ 50 cps, one must inject the projectile at a high speed, e.g., >500 m/s, to match the cycling time around the inner spiral. In this case a gun injector appears necessary, which in turn may require that the injection gun be mounted on a stationary (nongyrating) platform to avoid having the high gyrational gees interfere with the gun's operation.

Figure 7 shows such an arrangement in which the projectile is fired from a stationary gun through a transition section that leads into the gyrating spiral with a similar reverse transition at the spiral exit. This can be mechanically accomplished while maintaining projectile confinement to the guide-tube bore throughout the transition. For example, an elongated flexible drift tube could be used so that the end attached to the spiral executes the circular gyrational motion, and the other end executes a linear oscillatory motion parallel to the injection barrel. At the linear motion end a spline arrangement in which projections of the flexible drift tube slide back and forth in slots in the exit end of the barrel then completes the transition section.

Finally, we note that the gun must inject the projectile with a reproducible velocity into the stable quadrant of the inner spiral loop and within a time window substantially less than $1/4f$ s. The required low-jitter time and reproducible velocity can, for example, be accomplished using plasma jet ignition of chemical propellant guns.[5] For a repetitive-shot system, propellant gas from the injector (and the projectile's gas bearing) would have to be vented, e.g., through holes distributed along the inner side of the spiral tube opposite the gas bearing.

IV. Sled Friction Coefficients

For the slingatron to successfully accelerate a sled we need a friction coefficient that is sufficiently small that the Coriolis force exceeds the drag force for a small amplitude gyration, i.e.,

$$\mu < r\sin\theta/R << 1 \tag{39}$$

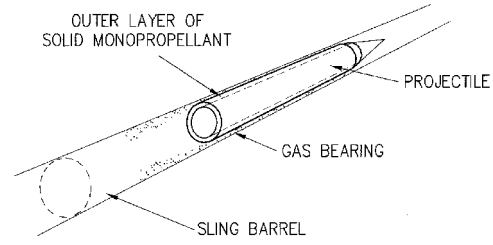

Fig. 8 Low-friction gas bearing generated by combustion of a sliding layer of monopropellant on the outside of a projectile.

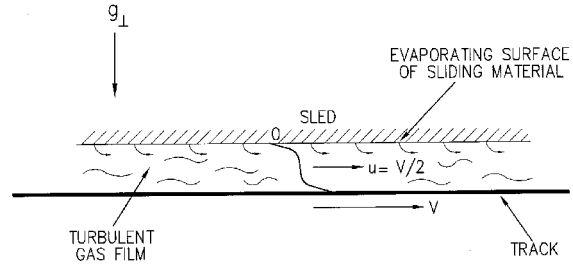

Fig. 9 Schematic of the gas flow in the bearing layer between the track and the sled.

In this section we discuss the use of a high-pressure gas film, supplied to the bearing layer between the underside of a sled and the track, which acts as a lubricant (Figs. 8 and 9). The advantages of a gas bearing are that a room-temperature steel track can be used (Fig. 2), and a high bearing pressure (and centrifugal force) can be supported. We consider two cases, namely, one in which the gas is stored or generated in a container in the sled and fed into the bearing, and one in which gas is supplied by an evaporating layer of solid material [possibly a layer of combustible monopropellant (Fig. 8)], on the underside of the sled. In both cases we only provide estimates based on assuming a simple Couette flow profile for the gas bearing in which the pressure gradient along the flow direction is negligible and the Reynolds number is large.[6,7]

A. Gas Stored or Generated in the Sled

In this case we assume that high-pressure gas is generated in a container inside the sled and injected into the bearing. For example this could be a container of cryogenic liquid, e.g., N_2 or H_2, that is stored in the sled and boiled off for injection into the bearing, or it could be a solid propellant that is burnt in a chamber to generate the needed gas. Gas from the bearing wake will accumulate in the guide tube and be re-encountered by the sled in the ring case (sometimes requiring removal), but not in the spiral case.

An estimate for the friction coefficient of a sled sliding on a high-pressure gas film can be obtained as follows. First, assume the gas film has a uniform thickness h, and note that for a gas film of pressure >50 bar, thickness $h \geq 10^{-3}$ cm, and sled velocity $\geq$ 1 km/s, the Reynolds number of the gas film is typically $\geq 1 \times 10^4$. The gas layer will thus be treated as turbulent with viscous sublayers adjacent to the sled and track surfaces, and a turbulent central flow with a flatter average velocity profile. Assuming the skin friction coefficients for the track and sled are equal, the skin drag force on the sled is approximately given by

$$F_{\parallel} = 0.5 c_f A \rho_{\text{gas}} V^2 \tag{40}$$

where ρ_{gas} is the gas density, c_f is the skin drag coefficient, and A is the sled's contact area with the gas film. We will use[8]

$$c_f = 0.45/(\log_{10} R_E)^{2.58} \tag{41}$$

The friction coefficient follows as

$$\mu = \frac{F_\parallel R}{mV^2} = \frac{\gamma}{2} c_f \left(\frac{V}{c_{gas}}\right)^2 \tag{42}$$

where we used $\rho_{gas} = \gamma P/c_{gas}^2$, with γ being the ratio of specific heats, $P = mV^2/RA$ is the gas pressure, and c_{gas} is the gas sound speed in the bearing. At low velocity the sound speed c_{gas} would approximately equal that of the gas at the track temperature, denoted as c_0, and at high sled velocity it is expected to approximately equal V. Thus, using a model $c_{gas}^2 = c_0^2 + V^2$ gives

$$\mu = \frac{\gamma}{2} c_f \frac{V^2}{(c_0^2 + V^2)} \tag{43}$$

which for $V^2 >> c_0^2$, gives an estimate $\mu \simeq 6 \times 10^{-3}$ for a Reynolds number of 3×10^4 and $\gamma = 1.3$.

Another important issue is surface heating. The steel track is exposed only briefly to the hot gas film as the sled passes a given point. However, the underside of the sled will be continuously exposed to the hot gas film and will at some velocity start to evaporate and contribute to the gas film. The case of an evaporatively supplied velocity bearing will be discussed in Sec. IV.B.

To estimate the track heating we need an expression for the convective heat transport to the track. This can be expressed in terms of the skin friction coefficient c_f by using the Reynolds analogy,[6] with the result

$$q_{wall} = 5 \times 10^3 c_f \left(\frac{V_{kls} P_{bars}}{\gamma - 1}\right) \frac{(T_{gas} - T_{wall})}{T_{gas}} \quad \text{W/cm}^2 \tag{44}$$

If we solve the thermal diffusion equation for a semi-infinite slab of steel with a constant heat flux q_{wall} arriving at its surface for a time $t = l/V$, where l is the length of the sled, one finds that the steel surface temperature rises by an amount

$$\Delta T_s(\text{K}) = \frac{2 q_{wall} t^{1/2}}{(\pi \rho_s c_s \kappa_s)^{1/2}} = 0.84 t^{1/2} q_{wall} \tag{45}$$

because of traversal by the sled's hot bearing gas, where ρ_s, c_s, and κ_s, are the mass density, specific heat, and thermal conductivity of the steel. For example, choosing $\gamma = 1.3$, $c_f = 6 \times 10^{-3}$, $P = 100$ bar, and $(T_{gas} - T_{wall})/T_{gas} \sim 0.5$, gives

$$\Delta T_s(\text{K}) = 132 (V_{kls} l_{meters})^{1/2} \tag{46}$$

This estimate predicts a tolerable temperature rise (for most cases) in the surface of the steel because of traversal by the sled. For the case in which both V and l are large it may become necessary to provide a protective thermal coating on the track surface.

B. Gas Derived from Evaporating or Combustible Monopropellant on the Sled Underside

At velocities above about 1 km/s, materials such as plastics sliding over a smooth steel track generate a thin film of hot gas at the sliding interface. The viscous power density in the high-velocity gradient across this gas film becomes sufficient to heat the gas and continuously evaporate the underside of the sled, thereby maintaining the gas bearing. Note also that the plastic could be chemically energetic (Fig. 8), with a pressure-dependent combustion rate to enhance the gas supply into the bearing, or simply to provide gas in the low-velocity range.

Thermal conduction beyond the evaporation layer into the sled interior is assumed slow because of the low thermal conductivity of the evaporating solids of interest, and the short surge acceleration time spent at high velocity in a ring accelerator or short traversal time through a spiral slingatron. The outblowing of evaporated gas from the sled underside will also reduce the turbulent convection of both thermal energy and momentum flux to that surface, which is a complex phenomenon requiring experimental data. However the following argument is made that it may be possible for an object to slide to extremely high velocity without being totally evaporated: First note that for constant μ the ratio (energy dissipated by friction)/(final kinetic energy) equals $\mu R/r \sin\theta$. We then assume that the sound speed of the bearing gas $c_s \simeq V$, so that its energy density per gram is $V^2/\gamma(\gamma - 1)$, and note that most of the frictional dissipation occurs as the projectile approaches its final velocity. The evaporated fraction would then be

$$\frac{\delta m}{m} \sim \frac{\gamma(\gamma - 1)}{2} \left(\frac{\mu R}{r \sin\theta}\right) \tag{47}$$

i.e., typically ~ 0.1.

V. Conclusions

The dynamics of ring and spiral slingatron mass accelerators has been further analyzed, and these accelerators appear to have a useful range of phase stability that would allow preprogrammed acceleration profiles. A gas bearing between the track and the sled provides an attractive means for obtaining the low friction coefficient needed to accelerate a sled (projectile) in the machine. It allows a room-temperature steel track to be used. The slingatron has a basic advantage for accelerating large masses to very high velocity, because the acceleration process is relatively slow (compared to EM railguns, coilguns, or mass drivers) and thus avoids the need for large pulsed power systems. The ring slingatron is essentially a mass synchrotron and the constant-frequency spiral slingatron is a mass cyclotron, and in both cases an accelerating Coriolis force proportional to m is used instead of an electric field force proportional to charge as in particle accelerators.

Potential applications include the ground-to-space launch of rocket projectiles, hypervelocity impact data, and various test range facilities. The spiral slingatron appears to have significant advantages for those applications in which it could be operated efficiently, for example cases requiring a constant input power for the launch of a continuing series of shots. Examples of such potential applications include rapid fire defense launchers, fuel injection into thermonuclear reactors, and propulsion.

Acknowledgments

The author wishes to thank several colleagues including Freeman Dyson, Princeton Institute of Advanced Study; John Hull, Argonne National Lab.; Liam Healy, Naval Research Lab.; D. S. Spicer, NASA–GSFC; and J. R. Greig, Slingatron Technologies, Inc., for useful discussions.

References

[1]Tidman, D. A., "Sling Launch of a Mass Using Superconducting Levitation," *IEEE Transactions on Magnetics*, Vol. 32, No. 1, 1996, pp. 240–247.

[2]Tidman, D. A., Burton, R. L., Jenkins, D. S., and Witherspoon, F. D., "Sling Launch of Materials into Space," *Proceedings of the 12th SSI/Princeton Conference on Space Manufacturing*, edited by B. Faughnan, Space Studies Inst., Princeton, NJ, 1995, pp. 59–70.

[3]Tidman, D. A., "Slingatron Dynamics and Launch to LEO," *Proceedings of the 13th SSI/Princeton Conference on Space Manufacturing*, edited by B. Faughnan, Space Studies Inst., Princeton, NJ, 1997, pp. 139–141.

[4]Eshbach, O. W., and Souders, M., *Handbook of Engineering Fundamentals*, 3rd ed., Wiley, New York, 1994, p. 516.

[5]Earnhart, J. R. D., Greig, J. R., Lilliott, E. L., Worthington, D., Buzzett, J., and McElroy, H. A., "A Comprehensive Model for Representing the Deterred Ball Powder Propellant WC885-0390 for Electrothermal-Chemical IBHVG2 Interior Ballistic Simulations," *Chemical Propulsion Information Agency Publication 606*, Vol. IV, Nov. 1993, pp. 51–63.

[6]Schlichting, H., *Boundary Layer Theory*, 7th ed., translated by J. Kestin, McGraw–Hill, New York, 1979.

[7]Thio, Y. C., Huerta, M. A., Boynton, G. C., Tidman, D, A., Wang, S. Y., and Winsor, N. K., "The Projectile-Wall Interface in Rail Launchers," *IEEE Transactions on Magnetics*, Vol. 29, No. 1, 1993, pp. 1213–1218.

[8]Fraas, A. P., and Ozisik, M. N., *Heat Exchanger Design*, Wiley, New York, 1965.